

Singlet and Triplet Excitation Management in a Bichromophoric Near-Infrared-Phosphorescent BODIPY-Benzoporphyrin Platinum Complex

Matthew T. Whited, Peter I. Djurovich, Sean T. Roberts, Alec C. Durrell,[†]
Cody W. Schlenker, Stephen E. Bradforth, and Mark E. Thompson*

Department of Chemistry, University of Southern California, Los Angeles,
California 90089, United States

Received September 20, 2010; E-mail: met@usc.edu

Abstract: Multichromophoric arrays provide one strategy for assembling molecules with intense absorptions across the visible spectrum but are generally focused on systems that efficiently produce and manipulate singlet excitations and therefore are burdened by the restrictions of (a) unidirectional energy transfer and (b) limited tunability of the lowest molecular excited state. In contrast, we present here a multichromophoric array based on four boron dipyrins (BODIPY) bound to a platinum benzoporphyrin scaffold that exhibits intense panchromatic absorption and efficiently generates triplets. The spectral complementarity of the BODIPY and porphyrin units allows the direct observation of fast bidirectional singlet and triplet energy transfer processes ($k_{ST}({}^1\text{BDP} \rightarrow {}^1\text{Por}) = 7.8 \times 10^{11} \text{ s}^{-1}$, $k_{TT}({}^3\text{Por} \rightarrow {}^3\text{BDP}) = 1.0 \times 10^{10} \text{ s}^{-1}$, $k_{TT}({}^3\text{BDP} \rightarrow {}^3\text{Por}) = 1.6 \times 10^{10} \text{ s}^{-1}$), leading to a long-lived equilibrated $[{}^3\text{BDP}][\text{Por}] \rightleftharpoons [\text{BDP}][{}^3\text{Por}]$ state. This equilibrated state contains approximately isoenergetic porphyrin and BODIPY triplets and exhibits efficient near-infrared phosphorescence ($\lambda_{em} = 772 \text{ nm}$, $\Phi = 0.26$). Taken together, these studies show that appropriately designed triplet-utilizing arrays may overcome fundamental limitations typically associated with core-shell chromophores by tunable redistribution of energy from the core back onto the antennae.

Introduction

The design of new chromophores for application in dye-sensitized and organic photovoltaic cells (OPVs) is an active area of research with important implications in energy science. Aside from meeting a variety of materials criteria, promising candidates must exhibit high absorptivities over a range of wavelengths to harvest the greatest possible fraction of available light. This criterion is critically important for devices employing organic thin films, for which exciton diffusion and carrier conduction can impose strict limits on the ideal thickness of active layers.¹ One promising strategy for achieving this goal is the construction of multichromophoric arrays capable of efficient intramolecular energy transfer between two or more highly absorbing components.² This approach has been used in a range of systems, in which “antenna” chromophores transfer energy to a central chromophore, reminiscent of the energy transfer relays in photosynthetic organisms such as purple

bacteria.³ Researchers have used dendrimers as synthetic mimics of these assemblies, with antennae arranged around central chromophores to optimize the energy transfer process, generating so-called core-shell systems with a “shell” of antenna chromophores surrounding a lower energy core.⁴ Although the core-shell approach can give good spectral coverage since both the core and shell absorbance can be used to excite the central chromophore, it often leads to isolation of the core chromophore, preventing effective energy-harvesting from the periphery of the core-shell system. Thus, while Förster processes can efficiently funnel energy to the interior, the insulating nature of the antennae effectively confines the excitation, preventing collection of charge or energy from the core. In this paper we report a core-shell system that efficiently captures a broad spectrum, using both antennae and core chromophores, and shows quantitative energy transfer from the antennae to core but at the same time spreads the excited state energy over both the core and shell chromophores. This has been achieved by selecting core and shell components having both the appropriate

[†] California Institute of Technology, Pasadena, CA 91125.

- (1) Peumans, P.; Yakimov, A.; Forrest, S. R. *J. Appl. Phys.* **2003**, *93*, 3693.
- (2) (a) Serin, J. M.; Brousmiche, D. W.; Frechet, J. M. J. *Chem. Commun.* **2002**, 2605. (b) Weil, T.; Reuther, E.; Mullen, K. *Angew. Chem., Int. Ed.* **2002**, *41*, 1900. (c) Cotlet, M.; Vosch, T.; Habuchi, S.; Weil, T.; Mullen, K.; Hofkens, J.; De Schryver, F. *J. Am. Chem. Soc.* **2005**, *127*, 9760. (d) Diring, S.; Puntoriero, F.; Nastasi, F.; Campagna, S.; Ziessel, R. *J. Am. Chem. Soc.* **2009**, *131*, 6108. (e) Kuciauskas, D.; Liddell, P. A.; Lin, S.; Johnson, T. E.; Weghorn, S. J.; Lindsey, J. S.; Moore, A. L.; Moore, T. A.; Gust, D. *J. Am. Chem. Soc.* **1999**, *121*, 8604. (f) Terazono, Y.; Kodis, G.; Liddell, P. A.; Garg, V.; Moore, T. A.; Moore, A. L.; Gust, D. *J. Phys. Chem. B* **2009**, *113*, 7147. (g) Li, X. Y.; Sinks, L. E.; Rybtchinski, B.; Wasielewski, M. R. *J. Am. Chem. Soc.* **2004**, *126*, 10810.

- (3) Hu, X. C.; Damjanovic, A.; Ritz, T.; Schulten, K. *Proc. Natl. Acad. Sci. U.S.A.* **1998**, *95*, 5935.
- (4) (a) Adronov, A.; Frechet, J. M. J. *Chem. Commun.* **2000**, 1701. (b) Denti, G.; Campagna, S.; Serroni, S.; Ciano, M.; Balzani, V. *J. Am. Chem. Soc.* **1992**, *114*, 2944. (c) Balzani, V.; Campagna, S.; Denti, G.; Juris, A.; Serroni, S.; Venturi, M. *Acc. Chem. Res.* **1998**, *31*, 26. (d) Stewart, G. M.; Fox, M. A. *J. Am. Chem. Soc.* **1996**, *118*, 4354. (e) Devadoss, C.; Bharathi, P.; Moore, J. S. *J. Am. Chem. Soc.* **1996**, *118*, 9635. (f) Sato, T.; Jiang, D. L.; Aida, T. *J. Am. Chem. Soc.* **1999**, *121*, 10658. (g) Choi, M. S.; Aida, T.; Yamazaki, T.; Yamazaki, I. *Angew. Chem., Int. Ed.* **2001**, *40*, 3194. (h) Frechet, J. M. J. *J. Polym. Sci., Part A: Polym. Chem.* **2003**, *41*, 3713.

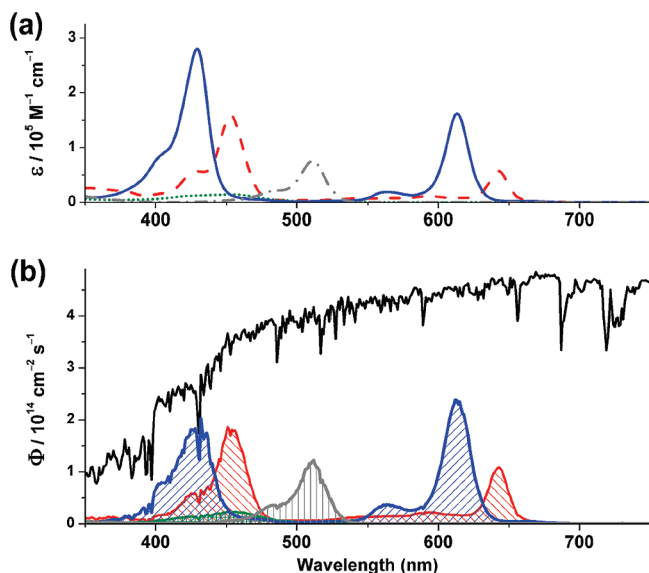
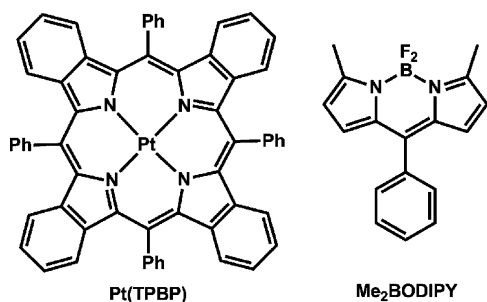


Figure 1. (a) UV-vis spectra of Pt(TPBP) (blue solid), chlorophyll B (red dash), Ru(bpy)₃²⁺ (green dot), and Me₂BODIPY (gray dot-dash). (b) Photon flux for AM1.5G (black) plotted with rate of photon absorption for 2 μ M solutions of Pt(TPBP) (blue), chlorophyll B (red), Ru(bpy)₃²⁺ (green), and Me₂BODIPY (gray dot-dash) in a 1-cm path length cell.

Chart 1. Model Complexes Used in This Study



singlet energies to promote efficient singlet energy transfer from shell to core and closely matched triplet energies to enable a balanced distribution of triplet energy between the core and shell.⁵

In addition to designing core and shell chromophores to achieve efficient singlet energy transfer and triplet equilibrium between the two components, it is important that the resultant complex has a net absorbance showing broad coverage across the solar spectrum. The importance and advantage of using complexes with panchromatic transitions may be readily demonstrated by comparing solar dyes in the context of solar radiation. In Figure 1a, UV-vis extinction spectra are presented for four chromophores: tris(bipyridyl)ruthenium(II); chlorophyll B;⁶ platinum tetraphenyltetrabenzoporphyrin (Pt(TPBP), Chart 1), a triplet material recently shown by our lab to perform well in lamellar OPVs;⁷ and Me₂BODIPY (Chart 1),⁸ a dye with an absorption spectrum complementary to that of Pt(TPBP).

Table 1. Visible-Light^a Absorption Properties of Representative Chromophores Referenced to AM1.5G Photon Flux⁹

complex	integrated absorption coefficient (M ⁻¹)	AM1.5G photon capture (1 μ M, 10 μ M) ^{a,b}	50% photon capture threshold (PCT ⁵⁰) ^{a,c}
Ru(bpy) ₃ ²⁺	0.70×10^8	0.9%, 7.7%	340 μ M
chlorophyll B	3.8×10^8	4.9%, 29%	29 μ M
Pt(TPBP)	6.2×10^8	7.0%, 32%	34 μ M
Me ₂ BODIPY	1.1×10^8	1.7%, 12%	490 μ M
Pt(TPBP) + 4Me ₂ BODIPY	11×10^8	13%, 53%	8.5 μ M

^a 350–750 nm. ^b Percentage of incident solar photons absorbed for a solution of a given concentration (1-cm path length). ^c Concentration required to absorb 50% of the incident solar photons (1-cm path length).

Pt(TPBP) and Me₂BODIPY are the two compounds we have chosen to use as the core and shell, respectively, in the light-harvesting system reported in this paper. In Figure 1b, the extinction spectra are translated into a rate of photon absorption under AM1.5G sunlight⁹ for a 2 μ M solution of each molecule.¹⁰ The percentage of photons absorbed can then be determined from the ratio of the integrated area under each curve to the integrated AM1.5G flux (black trace), which automatically corrects for the fact that photon flux varies with wavelength. Although the spectra in Figure 1 are plotted versus wavelength, it is important to note that the values presented in Table 1 were determined by integration versus energy rather than wavelength, since the inverse relationship between wavelength and energy will tend to overweight the lower-energy portion of the spectrum if wavelengths are used.

At low concentration, the percentage of photons absorbed roughly follows the integrated absorption coefficient (Table 1), and by this measure Pt(TPBP) appears to perform better than Ru(bpy)₃²⁺ and chlorophyll B. However, a more illuminating comparison is given by the 50% photon capture threshold (PCT⁵⁰), the concentration of a molecule required to absorb 50% of incident solar photons between 350 and 750 nm. The Pt(TPBP) complex exhibits a poorer PCT⁵⁰ than chlorophyll B because the relatively narrow transitions of the former span a comparatively small portion of the visible spectrum. Thus, with increasing concentration the absorbance of Pt(TPBP) at 450 and 620 nm quickly becomes saturated, whereas the absorbance between 450 and 550 nm is little improved.

Boron dipyrromethane (BODIPY) dyes such as Me₂BODIPY have been widely studied for imaging applications and exhibit high molar absorptivities in the 450–550 nm range,¹¹ precisely where absorption by Pt(TPBP) is weakest. In addition, since these molecules are intensely fluorescent between 500 and 600 nm, we hypothesized that Förster resonant energy transfer (FRET) from BODIPY to Pt(TPBP) would be fast and efficient, consistent with previous results showing that BODIPY chro-

(5) While the pioneering metallo dendrimers of Balzani^{4c} do easily access triplet excited states due to fast intersystem crossing at Ru and Os, energy transfer in these systems is still unidirectional, similar to singlet-based arrays.

(6) (a) Vernon, L. P.; Seely, G. R. *The Chlorophylls*; Academic Press: New York, 1966. (b) Kalyanasundaram, K. *Coord. Chem. Rev.* **1982**, 46, 159.

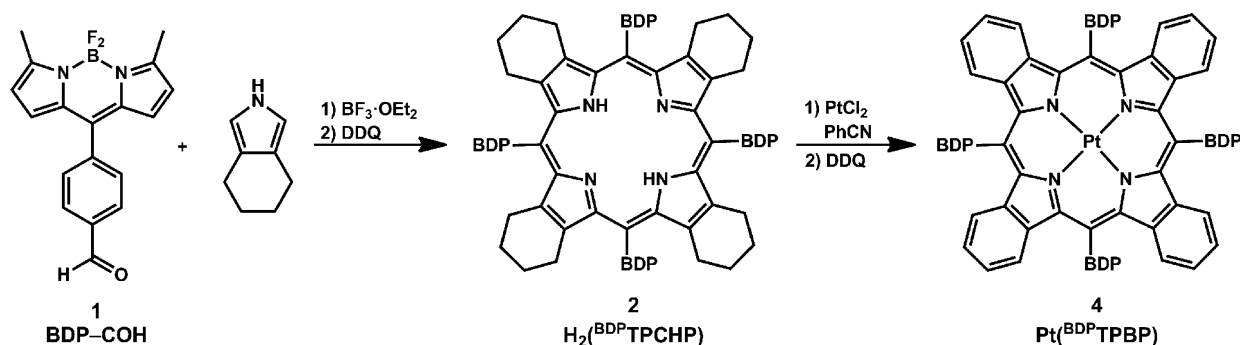
(7) (a) Perez, M. D.; Borek, C.; Djurovich, P. I.; Mayo, E. I.; Lunt, R. R.; Forrest, S. R.; Thompson, M. E. *Adv. Mater.* **2009**, 21, 1517. (b) Perez, M. D.; Borek, C.; Forrest, S. R.; Thompson, M. E. *J. Am. Chem. Soc.* **2009**, 131, 9281.

(8) Qin, W. W.; Baruah, M.; Van der Auweraer, M.; De Schryver, F. C.; Boens, N. J. *Phys. Chem. A* **2005**, 109, 7371.

(9) *ASTM Standard G173, Standard Tables for Reference Solar Spectral Irradiances: Direct Normal and Hemispherical on 37° Tilted Surface*; American Society for Testing and Materials: West Conshohocken, PA, 2008.

(10) A similar treatment has recently been used to describe absorption by neat films: Schlenker, C. W.; Thompson, M. E. *Chem. Commun.*, in press.

(11) (a) Ulrich, G.; Zissel, R.; Hariman, A. *Angew. Chem., Int. Ed.* **2008**, 47, 1184. (b) Loudet, A.; Burgess, K. *Chem. Rev.* **2007**, 107, 4891.

Scheme 1. Synthesis of Pt(BDP^{TPBP}) (4)

mophores can serve as effective antennae for porphyrins.^{2f,12} Employing parameters derived from model Me₂BODIPY and Pt(TPBP) complexes, and assuming random orientations and a separation of 10 Å, a high efficiency (>99.9%) and rate ($k_{\text{FRET}} = 8.3 \times 10^{11} \text{ s}^{-1}$) of FRET is predicted using the PhotochemCAD software package.¹³

As seen from Table 1, Me₂BODIPY exhibits lackluster PCT⁵⁰ properties by itself as a result of having only a single, sharp visible absorption band. However, if four Me₂BODIPY molecules are coupled to Pt(TPBP), the absorption bands of the two species are both balanced and complementary (Table 1), leading to dramatically improved PCT⁵⁰ values relative to Pt(TPBP) alone. Therefore, the combination of Pt(TPBP) and Me₂BODIPY chromophores into a single complex should lead to a multichromophoric array with UV–vis absorption properties that rival or exceed the best chromophores for solar energy harvesting (e.g., chlorophyll B). We report here the synthesis and photophysical study of such a complex consisting of one Pt(TPBP) and four Me₂BODIPY moieties in a core–shell arrangement. This multichromophoric complex efficiently absorbs across the visible spectrum, as illustrated in Figure 1 and Table 1, and at the same time gives the desirable energy transfer properties for core–shell materials described above, namely, funneling singlet energy to the core followed by rapid inter-system crossing and redistribution of the triplet state between the core and shell moieties.

Results and Discussion

Synthesis and Characterization of Pt(BDP^{TPBP}). The BODIPY–benzoporphyrin scaffold was assembled following the strategy of Finikova et al. (Scheme 1).¹⁴ Cyclohexenoporphyrin 2, with four BODIPY units connected to the *meso* positions by phenylene linkers, was accessed in 35% yield via an acid-catalyzed macrocyclization of 4,5,6,7-tetrahydroisoidole and

BODIPY derivative 1 with a *para* aldehyde functionality.¹⁵ Platination and oxidation of 2 were performed as previously described for the related Pt(TPBP) complex,¹⁶ ultimately affording 4 in pure form as a dark green-black solid in 10% yield over two steps (see Experimental Section for full synthetic details).

The UV–vis spectrum of 4 is presented in Figure 2 along with the spectrum predicted from Pt(TPBP) and four Me₂BODIPY model complexes. As expected, the absorption profile of 4 is a composite of those for the model complexes, with exceptionally intense transitions across the visible spectrum. Although the peak at 514 nm ascribed to the BODIPY units is quite similar to that of Me₂BODIPY, the Soret and Q peaks characteristic of the benzoporphyrin are broadened relative to Pt(TPBP). For instance, the Soret band at 433 nm exhibits a full width at half-maximum (fwhm) of 35 nm, compared with 22 nm for Pt(TPBP), and the fwhm for the Q-band at 619 nm has increased from 19 nm for Pt(TPBP) to 24 nm for 4. The porphyrin peak broadening may be due to conformational disorder and the accompanying molecular distortion of the BODIPY units.^{12a,17} This broadening leads to a small improvement in photon capture properties relative to those predicted for 4 (AM1.5G Photon Capture (1 μM) = 14% (measured), 13% (predicted); PCT⁵⁰ = 7.0 μM (measured), 8.5 μM (predicted)), though the integrated absorption coefficient is unchanged.

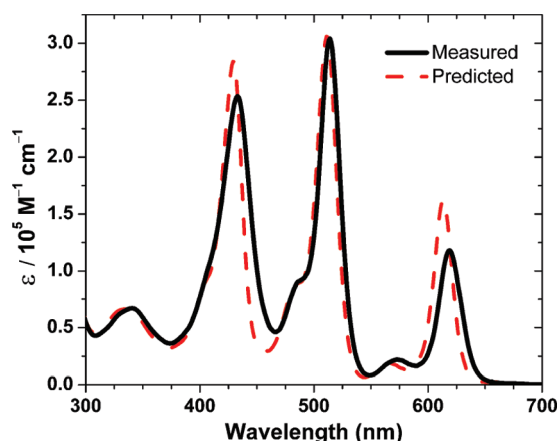


Figure 2. Predicted (dashed) and measured (solid) UV–vis spectra for 4 in CH₂Cl₂.

Panchromatic absorption in a multichromophoric array is only useful if efficient energy transfer between the components can be realized, so we turned to photoluminescence (PL) measurements to examine the fate of absorbed photons. At room

- (12) (a) Li, F. R.; Yang, S. I.; Ciringh, Y. Z.; Seth, J.; Martin, C. H.; Singh, D. L.; Kim, D. H.; Birge, R. R.; Bocian, D. F.; Holten, D.; Lindsey, J. S. *J. Am. Chem. Soc.* **1998**, *120*, 10001. (b) Lee, C. Y.; Hupp, J. T. *Langmuir* **2010**, *26*, 3760. (c) Koepf, M.; Trabolsi, A.; Elhabiri, M.; Wytko, J. A.; Paul, D.; Albrecht-Gary, A. M.; Weiss, J. *Org. Lett.* **2005**, *7*, 1279. (d) Kumaresan, D.; Datta, A.; Ravikanth, M. *Chem. Phys. Lett.* **2004**, *395*, 87. (e) Maligaspe, E.; Tkachenko, N. V.; Subbaiyan, N. K.; Chitta, R.; Zandler, M. E.; Lemmetyinen, H.; D'Souza, F. J. *Phys. Chem. A* **2009**, *113*, 8478. (f) Ambrose, A.; Wagner, R. W.; Rao, P. D.; Riggs, J. A.; Hascoat, P.; Diers, J. R.; Seth, J.; Lammi, R. K.; Bocian, D. F.; Holten, D.; Lindsey, J. S. *Chem. Mater.* **2001**, *13*, 1023. (g) Lammi, R. K.; Wagner, R. W.; Ambrose, A.; Diers, J. R.; Bocian, D. F.; Holten, D.; Lindsey, J. S. *J. Phys. Chem. B* **2001**, *105*, 5341.
- (13) Du, H.; Fuh, R. C. A.; Li, J. Z.; Corkan, L. A.; Lindsey, J. S. *Photochem. Photobiol.* **1998**, *68*, 141.
- (14) Finikova, O. S.; Cheprakov, A. V.; Beletskaya, I. P.; Carroll, P. J.; Vinogradov, S. A. *J. Org. Chem.* **2003**, *69*, 522.

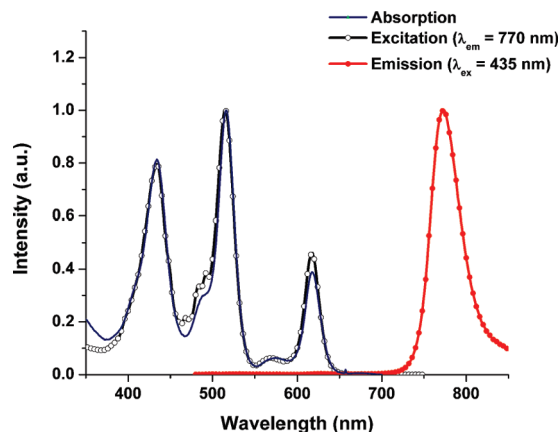


Figure 3. Normalized absorption, excitation ($\lambda_{\text{em}} = 770$ nm), and emission ($\lambda_{\text{ex}} = 435$ nm) spectra of **4** in toluene.

temperature in toluene, irradiation of the porphyrin at 435 nm leads to near-infrared (NIR) phosphorescence ($\lambda_{\text{em}} = 772$, Figure 3) along with extremely weak porphyrin fluorescence ($\lambda_{\text{em}} = 628$ nm, $\Phi_{\text{fl}} < 0.001$), similar to what has previously been reported for metal–benzoporphyrin complexes.^{14,16,18} An excitation spectrum for this 772 nm emission closely parallels the absorption spectrum of **4** (Figure 3), indicating that intramolecular energy transfer is quite efficient, as expected. Thus, direct excitation of the BODIPY subunit at 500 nm results in nearly exclusive (>98%) phosphorescent emission at 772 nm.

Recent studies have indicated that the triplet state of BODIPY resides close in energy to the observed emission at 772 nm, suggesting that the lowest-lying excited state of BODIPY–benzoporphyrin hybrids may be precisely controlled by independent tuning of the BODIPY and porphyrin subunits.¹⁹ However, the phosphorescence efficiency (26%) and lifetime ($\tau = 67$ μs) in toluene are similar to those previously reported for platinum benzoporphyrins,^{16,20} as opposed to much lower efficiencies and millisecond lifetimes reported for sensitized triplet emission from the organic BODIPY fragment.^{19a} Therefore, we assign emission to phosphorescence from the platinated benzoporphyrin moiety. Nevertheless, the influence of the nonemissive BODIPY triplet on the excited state properties is still considerable (vide infra).

The behavior of **4** in rigid matrices closely parallels what is observed in fluid solution. At 77 K in 2-methyltetrahydrofuran (2-MeTHF), a single intense NIR phosphorescent emission is observed at 764 nm ($\tau = 92$ μs), with quantitative BODIPY \rightarrow porphyrin energy transfer (Figure S5 in Supporting Information).

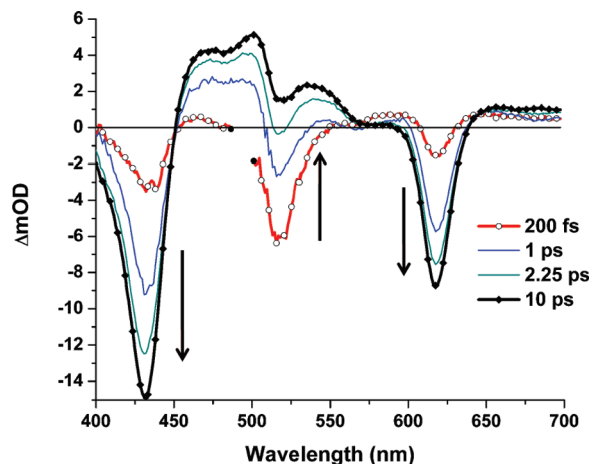


Figure 4. Ultrafast transient absorption spectra of **4** in toluene after excitation at 508 nm (0.2–10 ps) (N.B.: solvent response at short time delays prevents the accurate collection of data from 480 to 500 nm, so these data points have been omitted from the 200 fs trace above).

The PL behavior of **4** doped (0.5%) into a poly(methyl methacrylate) (PMMA) matrix is analogous, with efficient energy transfer and long lifetimes ($\tau = 95$ μs), though the quantum efficiency ($\Phi = 0.17$) is slightly lower than in fluid toluene solution due to a decreased radiative decay rate ($k_{\text{r}} = 3.9 \times 10^3$ s^{-1} in toluene, 1.8×10^3 s^{-1} in PMMA; $k_{\text{nr}} = 1.1 \times 10^4$ s^{-1} in toluene, 8.7×10^3 in PMMA). Neat films of **4**, on the other hand, only display a broad, red-shifted emission (935 nm) at 77 K (Figure S8 in Supporting Information), indicating competitive deactivation in the neat solid by excimer formation, as previously observed for Pt(TPBP).^{7a}

Femtosecond Transient Absorption: Observation of Bidirectional Singlet and Triplet Energy Transfer. Steady-state PL measurements show that irradiation of **4** leads to benzoporphyrin-based phosphorescence but reveal no details of the energy-transfer processes that precede emission. In particular, upon formation of the BODIPY singlet excited state (^1BDP), the porphyrin triplet state (^3Por) can be populated by (a) $^1\text{BDP} \rightarrow ^1\text{Por}$ singlet energy transfer (ST) followed by intersystem crossing (ISC) to give ^3Por or (b) rapid intersystem crossing at BODIPY to form ^3BDP , followed by triplet energy transfer (TT) to give ^3Por . Results from both our laboratory²¹ and others²² have shown that the ISC rate for Pt(TPBP) is 2.5×10^{12} s^{-1} ($\tau = 400$ fs). On the other hand, time-resolved studies have also shown that the ISC rate for BODIPY derivatives in the absence of a heavy atom is quite slow ($k_{\text{ISC}} < 2 \times 10^8$ s^{-1}).¹⁷ It is thus likely that $^1\text{BDP} \rightarrow ^1\text{Por}$ energy transfer precedes ISC, but steady-state measurements cannot rule out the alternative possibility of ISC prior to energy transfer.

We set out to discriminate between these two pathways by using ultrafast transient absorption to observe energy transfer and intersystem crossing events occurring within the first hundred picoseconds of excitation. These studies lead to the observation of two distinct energy-transfer processes. First, upon selective excitation of BODIPY at 508 nm, a bleach at 515 nm is observed within 200 fs due to the formation of ^1BDP . The 515 nm bleach recovers over a period of ca. 10 ps, accompanied by a simultaneous growth of bleaches at 450 and 620 nm that correspond to the benzoporphyrin Soret and Q bands, respectively (Figure 4). A global fit to the data yields a rate for $^1\text{BDP} \rightarrow ^1\text{Por}$ singlet energy transfer of $1/k_{\text{ST}} = 1.29 \pm 0.11$ ps (Figure 5b), which is quite similar to the rate predicted for FRET using model Me_2BODIPY and Pt(TPBP)

- (15) (a) Miao, Q.; Shin, J.-Y.; Patrick, B. O.; Dolphin, D. *Chem. Commun.* **2009**, 2541. (b) Shin, J. Y.; Tanaka, T.; Osuka, A.; Miao, Q.; Dolphin, D. *Chem.—Eur. J.* **2009**, *15*, 12955.
- (16) Borek, C.; Hanson, K.; Djurovich, P. I.; Thompson, M. E.; Aznavour, K.; Bau, R.; Sun, Y.; Forrest, S. R.; Brooks, J.; Michalski, L.; Brown, J. *Angew. Chem., Int. Ed.* **2007**, *46*, 1109.
- (17) Kee, H. L.; Kirmaier, C.; Yu, L. H.; Thamyongkit, P.; Youngblood, W. J.; Calder, M. E.; Ramos, L.; Noll, B. C.; Bocian, D. F.; Scheidt, W. R.; Birge, R. R.; Lindsey, J. S.; Holten, D. *J. Phys. Chem. B* **2005**, *109*, 20433.
- (18) Lebedev, A. Y.; Filatov, M. A.; Cheprakov, A. V.; Vinogradov, S. A. *J. Phys. Chem. A* **2008**, *112*, 7723.
- (19) (a) Galletta, M.; Campagna, S.; Quesada, M.; Ulrich, G.; Ziesse, R. *Chem. Commun.* **2005**, 4222. (b) Rachford, A. A.; Ziesse, R.; Bura, T.; Retaillieu, P.; Castellano, F. N. *Inorg. Chem.* **2010**, *49*, 3730. (c) Singh-Rachford, T. N.; Haefele, A.; Ziesse, R.; Castellano, F. N. *J. Am. Chem. Soc.* **2008**, *130*, 16164.
- (20) Borisov, S. M.; Papkovsky, D. B.; Ponomarev, G. V.; DeToma, A. S.; Saf, R.; Klimant, I. *J. Photochem. Photobiol., A* **2009**, *206*, 87.

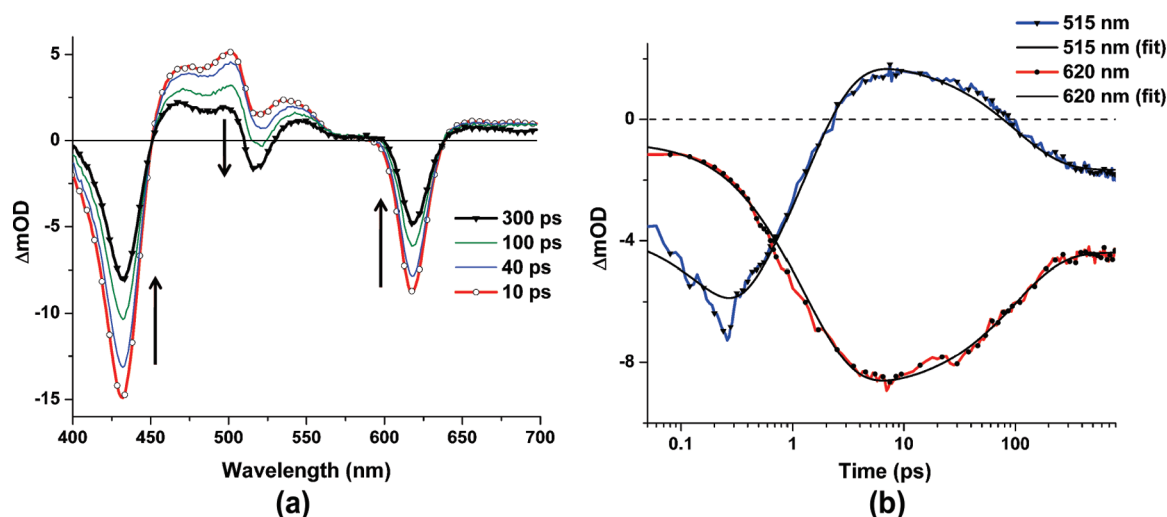


Figure 5. (a) Ultrafast transient absorption spectra of **4** after excitation at 508 nm (10–300 ps). (b) Time domain slices of transient absorptions at 515 nm (BODIPY) and 620 nm (porphyrin) with predicted traces based on kinetic parameters for the system.

complexes ($1/k_{\text{FRET}} = 1.2$ ps, vide supra). The transient spectrum obtained after 10 ps closely resembles spectra reported for the Pt(TPBP) triplet,^{21–23} consistent with previous measurements revealing a rate of intersystem crossing for Pt(TPBP) of $1/k_{\text{ISC}} = 400$ fs and indicating that the generation of ^1Por by ST from ^1BDP is followed by fast and quantitative intersystem crossing to produce ^3Por .

At longer times (10–300 ps, Figure 5a) the bleach signals for ^3Por decrease, accompanied by a concomitant partial return of the BODIPY bleach at 515 nm. These spectral changes are assigned to $^3\text{Por} \rightarrow ^3\text{BDP}$ triplet energy transfer and were modeled to afford a transfer rate of $1/k_{\text{F}} = 99.6 \pm 7.1$ ps. The triplet transfer/exchange process establishes an equilibrated $^3\text{BDP}[\text{Por}] \rightleftharpoons [\text{BDP}][^3\text{Por}]$ state in ca. 300 ps that does not develop further on the time-scale of the experiment (800 ps). The interplay between BODIPY and porphyrin excited states following selective BODIPY excitation is illustrated in Figure 5b, where the transient absorptions at 515 nm (BODIPY) and 620 nm (porphyrin) are plotted versus time, along with fits associated with the kinetic parameters presented above. The 50% recovery of the Soret and Q bleaches from 10 to 800 ps supports roughly equal populations of the ^3BDP and ^3Por states several hundred picoseconds after excitation and indicates a redistribution of energy from the porphyrin core back onto BODIPY antennae in the form of a triplet excited state. This hypothesis is supported by the fact that the transient spectrum obtained at 300 ps exhibits the combined features of spectra reported for the triplet of the Pt(TPBP) model complex^{22,23} and closely related BODIPY triplets.^{19b,24}

Nanosecond-to-Microsecond Transient Absorption: Characterization of an Equilibrated Emissive State.

To further examine the interplay of BODIPY and platinum porphyrin triplet states observed by femtosecond transient absorption, we turned to nanosecond-resolved TA measurements to elucidate the nature of the long-lived, phosphorescent state of **4**. As shown in Figure 6a, excitation of the BODIPY moiety at 487 nm leads to a transient absorption spectrum that is dominated by bleaches corresponding to the benzoporphyrin Soret and Q bands (435 and 620 nm, respectively) but also contains a distinct bleach of the BODIPY absorbance (515 nm) and is essentially unchanged from the spectra recorded at 800 ps (vide supra). All features in the transient spectrum decay at the same rate, which matches the rate of phosphorescent decay ($\lambda_{\text{em}} = 768$ nm) measured for the same solution (Figure 6b). Taken together, these findings show that the long-lived state generated upon excitation of BODIPY consists of BODIPY and benzoporphyrin triplets that reach thermal equilibrium within several hundred picoseconds of excitation. Since the energy transfer leading to equilibration of the triplets (10^{10} s^{-1}) is much faster than phosphorescent decay (10^{10} s^{-1}), the ratio of the species remains constant over the phosphorescent lifetime.

The observation of fast thermal equilibration of the triplet states allows two calculations to be made regarding the dynamics of the molecule. First, the thermal equilibrium between porphyrin triplet (^3Por) and BODIPY triplet (^3BDP) may be described using a Boltzmann distribution, allowing the energy of ^3BDP to be estimated if the relative populations of ^3Por and ^3BDP are known. The energy difference between two states in thermal equilibrium is given by²⁵

$$\Delta E = E_2 - E_1 = kT \ln \left(\frac{d_1 P_2}{d_2 P_1} \right) \quad (1)$$

where d_n represents the degeneracy of state n , and P_n represents the population of state n . Since there are four BODIPY antennae surrounding the porphyrin core, we regard the ^3BDP state as

- (21) Roberts, S. T.; Schlenker, C. W.; Barlier, V.; McAnally, R. E.; Zhang, Y.; Mastron, J. N.; Thompson, M. E.; Bradforth, S. E. *J. Phys. Chem. Lett.*, submitted for publication.
- (22) Rajapakse, G. V. N. *Photophysical Properties of Metallotetraphenyltetraazaporphyrins: Insights from Experimental and Theoretical Studies*. Ph.D. Thesis; Bowling Green State University: Bowling Green, OH, 2008.
- (23) Singh-Rachford, T. N.; Castellano, F. N. *Inorg. Chem.* **2009**, *48*, 2541.
- (24) Although the triplet of the Me_2BODIPY model complex could not be observed because of inefficient intersystem crossing, a closely related BODIPY triplet could be quantitatively generated in unoxidized intermediate **3**, for which the BODIPY triplet (which is identical to that in complex **4**) is much lower in energy than the porphyrin triplet. The transient absorption spectra of **3** are provided in the Supporting Information (Figures S12 and S13) as a model for the contributions of ^3BDP to the transient absorption spectra of complex **4**.

- (25) The derivation of this equation is presented in the Supporting Information.

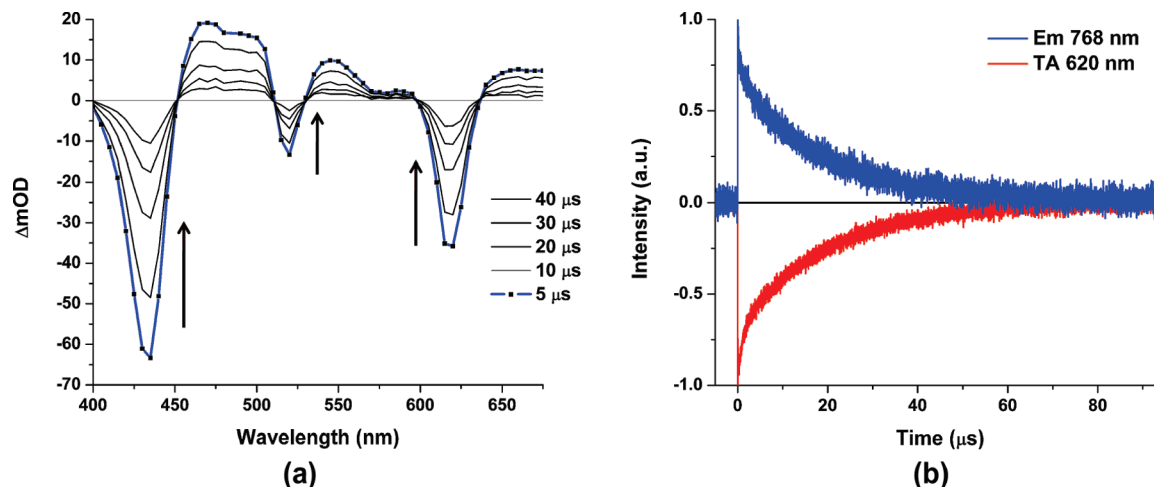


Figure 6. (a) Nanosecond transient absorption spectra of **4** following excitation at 487 nm. (b) Normalized phosphorescent decay of **4** and restoration of bleach at 620 nm, monitored by time-resolved transient absorption spectroscopy.

quadruply degenerate,^{26,27} whereas ³Por is doubly degenerate due to its ³E_g state,^{22,28} giving ($d_{\text{BDP}}/d_{\text{Por}} = 2$). The relative equilibrium populations of ³Por and ³BDP were estimated to be 0.45 and 0.55, respectively, after scaling the observed bleaches by the respective extinction coefficients for the BODIPY and benzoporphyrin portions of complex **4** and keeping in mind that the ground-state absorption attributed to BODIPY corresponds to the absorption of four BODIPY units. From these populations, ΔE was calculated to be $0.5kT$, or 12 meV under experimental conditions ($T = 293$ K), confirming that the two triplets are nearly isoenergetic. The energy of ³Por, derived from the emission maximum at 77 K, is 1.62 eV (764 nm). On the basis of these calculations, the energy of ³BDP is estimated to be 1.64 eV (758 nm), quite similar to values reported for phosphorescence from related BODIPY chromophores.^{19a,b} These values are also supported by the ca. 50% restoration of the bleaches corresponding to ³Por between 10 and 800 ps mentioned above. Additional support for the energy of ³BDP in complex **4** is provided by PL measurements of the unoxidized platinum cyclohexenoporphyrin **3** that was isolated as an intermediate in the synthesis of **4**. Although **3** is nonemissive at room temperature, phosphorescence is exclusively observed at 756 nm at 77 K (Figure S4 in Supporting Information). This emission, which is significantly lower in energy than those previously reported for metalated cyclohexenoporphyrins,¹⁸ has been assigned to BODIPY phosphorescence and is nearly identical to the energy determined using eq 1.

Second, the thermal equilibrium between ³BDP and ³Por excited states leads to an “energy reservoir” effect, similar to that previously described for polycyclic aromatic hydrocarbons (e.g., pyrene, naphthalene) attached to metal complexes.^{27,29} This effect leads to a lengthening of the observed lifetime according to the following equation when the states are in rapid equilibrium:

$$\frac{1}{\tau_{\text{obs}}} = \frac{P_1}{\tau_1} + \frac{P_2}{\tau_2} \quad (2)$$

where P_n and τ_n represent, respectively, the relative population and lifetime of state n . Based on the relative populations of ³BDP and ³Por determined above and assuming that $\tau_{\text{BDP}} \gg \tau_{\text{Por}}$, the observed lifetime of 67 μs in dilute toluene represents a 37 μs extension relative to the phosphorescent lifetime expected for the porphyrin in the absence of an energy reservoir (30 μs). This calculated lifetime is quite close to values recently reported by Borisov et al. for related platinum benzoporphyrin complexes,²⁰ adding credence to the estimation of the relative populations of ³BDP and ³Por states and thus to the projected energy of ³BDP.

The combination of femtosecond and nanosecond TA studies with steady-state experiments allows construction of a Jablonski diagram describing the excited-state behavior of Pt(^{BDP}TPBP) (**4**) (Figure 7, Table 2). After irradiation of the BODIPY fragment to form ¹BDP, Förster energy transfer generates an excited singlet state (¹Por) on the platinated benzoporphyrin. Rapid intersystem crossing to ³Por and overlap with the photobleach of the BODIPY unit render ¹Por invisible to our transient absorption experiments. However, the energy of this state can be determined from the observed fluorescent emission at 628 nm, which is very weak ($\Phi < 0.001$) as a result of the extremely efficient ISC. Following intersystem crossing, thermal equilibration occurs between the close-lying ³Por and ³BDP states, that is, an *efficient redistribution of excitation energy from core to shell*. Since the lifetime of the ³BDP state greatly exceeds that of ³Por, the decay of this equilibrated state is governed by the relative energies of these states (and consequently their relative populations) as well as the lifetime of ³Por.

Balzani and co-workers have investigated unidirectional Dexter-type triplet energy transfer between ruthenium and osmium polypyridyl complexes through rigid oligophenylene linkers.³⁰ For their system, the rate of triplet energy transfer was found to be related to the number of intervening phenylene units according to the equation

$$k_{\text{TT}} \propto e^{-\gamma n} \quad (3)$$

where n is the number of phenylene units and γ is an attenuation constant. An extension of their regression to $n = 1$ predicts a

(26) This predicted equilibrium shift upon adding multiple degenerate energy reservoirs has been experimentally verified for Ru(bpy)₃-pyrene systems (ref 27).

(27) (a) Tyson, D. S.; Castellano, F. N. *J. Phys. Chem. A* **1999**, *103*, 10955. (b) Tyson, D. S.; Henbest, K. B.; Bialecki, J.; Castellano, F. N. *J. Phys. Chem. A* **2001**, *105*, 8154. (c) McClenaghan, N. D.; Barigelletti, F.; Maubert, B.; Campagna, S. *Chem. Commun.* **2002**, 602.

(28) Gouterman, M. In *The Porphyrins*; Dolphin, D., Ed.; Academic Press: New York, 1978; Vol. 3, p 1.

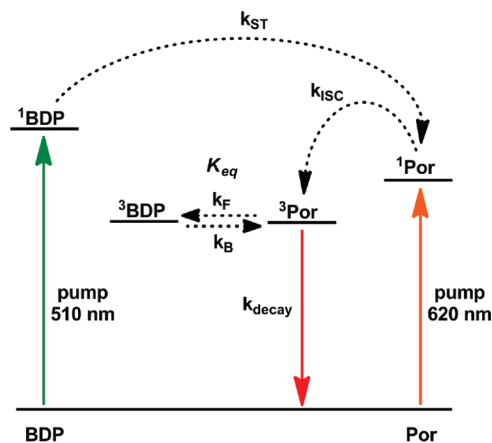


Figure 7. Jablonski diagram summarizing the excited-state behavior of Pt(BDP)TPBP (**4**) upon selective irradiation of the BODIPY or benzoporphyrin units.

Table 2. Measured Rate Constants and Energy Levels for Figure 7

k_{ST} ($^1\text{BDP} \rightarrow ^1\text{Por}$)	$7.8 \times 10^{11} \text{ s}^{-1}$
k_{ISC} (Por)	$2.5 \times 10^{12} \text{ s}^{-1}$
k_F ($^3\text{Por} \rightarrow ^3\text{BDP}$)	$1.0 \times 10^{10} \text{ s}^{-1}$
k_B ($^3\text{BDP} \rightarrow ^3\text{Por}$)	$1.6 \times 10^{10} \text{ s}^{-1}$
$k_{\text{decay}} = k_r + k_{nr}$	$1.5 \times 10^5 \text{ s}^{-1}$
$K_{eq} = k_F/k_B$	0.61
$E(^1\text{BDP})$	2.41 eV (516 nm)
$E(^1\text{Por})$	2.00 eV (622 nm)
$E(^3\text{BDP})$	1.64 eV (758 nm)
$E(^3\text{Por})$	1.62 eV (764 nm)

triplet energy transfer rate (k_{TT}) of $1.1 \times 10^{10} \text{ s}^{-1}$, nearly identical to the value we observe for $k_{TT}(^3\text{BDP} \rightarrow ^3\text{Por})$ of $1.6 \times 10^{10} \text{ s}^{-1}$. This finding indicates that triplet energy transfer between the benzoporphyrin and BODIPY moieties in **4** likely occurs across the phenylene linker via a superexchange mechanism in a process similar to that described by Balzani for the polypyridyl complexes.

Consequences of Using Multichromophoric Arrays for Triplet Generation. The efficient energy cascade depicted in Figure 7 renders complex **4** analogous to the “cascadellies” developed by Ulrich, Ziessel, and co-workers, that are used to increase the apparent Stokes shifts of BODIPY fluorophores.³¹ In our case, the combination of intense panchromatic absorption with bidirectional intramolecular energy transfer makes the resulting phosphorescent cascabelle a unique example of a core–shell chromophore capable of efficiently funneling energy to the core followed by redistribution back onto the antennae.

This unusual set of interactions is made possible by the different singlet–triplet gaps associated with the BODIPY and benzoporphyrin moieties, which allow the behavior of this lowest-energy molecular excited state to be tuned without disturbing the complementary ground-state absorption properties of the ensemble. In light of recent results from our laboratory suggesting that molecules with excited states residing largely on the periphery may exhibit improved performance in organic electronics,³² such a property may prove highly desirable.

Unfortunately, as mentioned above, neat films of **4** only exhibit excimer emission at 77 K, indicating an energy loss pathway for this particular molecule that renders it less desirable as a donor for lamellar solar cells. At the moment, it is not clear whether this emission is attributable to BODIPY- or porphyrin-centered excimers. Nevertheless, the findings reported in this paper have shown that modest tuning of the singlet–triplet gap for one of the units may disfavor this sort of deactivation.

Conclusions

In conclusion, we have synthesized and characterized a NIR-phosphorescent BODIPY-platinabenzoporphyrin hybrid complex that exhibits broad visible-light absorption, fast and efficient intramolecular energy transfer, and high PL efficiencies up to 26% at ambient temperature in fluid solution. Using femto- and nanosecond transient absorption spectroscopy, we have elucidated bidirectional singlet and triplet energy transfer pathways for the array, leading to a long-lived, equilibrated [^3BDP][Por] \rightleftharpoons [BDP][^3Por] state due to the nearly isoenergetic BODIPY and benzoporphyrin triplets. As a result, the hybrid complex may be described as an unusual example of a core–shell chromophore that overcomes the normal limitation of unidirectional energy transfer by utilizing singlets to funnel excitation energy into the core and triplets to redistribute it back onto the antennae. Castellano and co-workers have amply demonstrated the potential importance of intermolecular singlet–triplet interactions through recent investigations of photon upconversion by triplet–triplet annihilation.^{19c,33} In this paper, we have shown that intramolecular singlet–triplet interactions may be utilized for a different purpose, allowing fine-tuning of energy-transfer pathways in multichromophoric arrays through careful modification of the singlet–triplet gaps of the constituent materials to couple efficient light absorption with efficient bidirectional energy redistribution. Future work will be aimed at modifying the properties of such triplet-utilizing arrays to optimize their performance in organic photovoltaics.

Experimental Section

General Considerations. 4,4-Difluoro-3,5-dimethyl-8-(4-formylphenyl)-4-bora-3a,4a-diaza-s-indacene (**1**) was prepared by the method of Dolphin and co-workers.^{15a} All other reagents were purchased from commercial vendors and used without further purification. All air-sensitive manipulations were performed using standard Schlenk techniques as needed, following the procedures indicated below for each preparation. NMR spectra were recorded at ambient temperature on Varian Mercury 500 and 600 MHz spectrometers; ^1H chemical shifts were referenced to residual solvent. UV–vis spectra were recorded on a Hewlett-Packard 4853 diode array spectrophotometer. Steady-state emission experiments at room temperature and 77 K as well as phosphorescence decays were performed using a Photon Technology International Quanta-

- (29) (a) Ford, W. E.; Rodgers, M. A. J. *J. Phys. Chem.* **1992**, *96*, 2917. (b) Rachford, A. A.; Goeb, S.; Ziessel, R.; Castellano, F. N. *Inorg. Chem.* **2008**, *47*, 4348. (c) Hissler, M.; Harriman, A.; Khatyr, A.; Ziessel, R. *Chem.–Eur. J.* **1999**, *5*, 3366. (d) Morales, A. F.; Accorsi, G.; Armaroli, N.; Barigelletti, F.; Pope, S. J. A.; Ward, M. D. *Inorg. Chem.* **2002**, *41*, 6711. (e) Leroy-Lhez, S.; Belin, C.; D’Aleo, A.; Williams, R. M.; De Cola, L.; Fages, F. *Supramol. Chem.* **2003**, *15*, 627. (f) Ziessel, R.; Hissler, M.; El-Ghayoury, A.; Harriman, A. *Coord. Chem. Rev.* **1998**, *178*, 1251. (g) Tyson, D. S.; Luman, C. R.; Zhou, X. L.; Castellano, F. N. *Inorg. Chem.* **2001**, *40*, 4063. (h) Lavie-Cambot, A.; Lincheneau, C.; Cantuel, M.; Leydet, Y.; McClenaghan, N. D. *Chem. Soc. Rev.* **2010**, *39*, 506. (i) Medlycott, E. A.; Hanan, G. S.; Loiseau, F.; Campagna, S. *Chem.–Eur. J.* **2007**, *13*, 2837.
- (30) Schlicke, B.; Belser, P.; De Cola, L.; Sabbioni, E.; Balzani, V. *J. Am. Chem. Soc.* **1999**, *121*, 4207.
- (31) (a) Ulrich, G.; Goze, C.; Guardigli, M.; Roda, A.; Ziessel, R. *Angew. Chem., Int. Ed.* **2005**, *44*, 3694. (b) Goze, C.; Ulrich, G.; Ziessel, R. *J. Org. Chem.* **2007**, *72*, 313.

- (32) Wu, C.; Djurovich, P. I.; Thompson, M. E. *Adv. Funct. Mater.* **2009**, *19*, 3157.
- (33) Singh-Rachford, T. N.; Nayak, A.; Muro-Small, M. L.; Goeb, S.; Therien, M. J.; Castellano, F. N. *J. Am. Chem. Soc.* **2010**, *132*, 14203.

Master Model C-60SE spectrofluorimeter. Quantum efficiency measurements were carried out using a Hamamatsu C9920 system equipped with a xenon lamp, calibrated integrating sphere, and model C10027 photonic multichannel analyzer.

Cyclohexenoporphyrin 2·(HCl)₂ [H₄(^{BDP}TPCHP)Cl₂]. In a 3-neck round-bottom flask, dichloromethane (125 mL) was sparged with N₂ with stirring for 20 min. The flask was shielded from light, 4,5,6,7-tetrahydroisindole (54 mg, 0.45 mmol) and aldehyde **1** (157 mg, 0.48 mmol) were added as solids, and the solution was stirred under N₂ for 10 min. BF₃·OEt₂ (20 μ L, 0.10 mmol) was added via syringe, and the resulting mixture was stirred for 2.5 h. DDQ (127 mg, 0.56 mmol) was added in one portion, and the reaction was allowed to proceed with stirring for 18 h. The resulting red-brown solution was washed with 10% aq. Na₂SO₃ (3 \times 50 mL) and brine (1 \times 75 mL), dried (MgSO₄), filtered, and concentrated in vacuo to a brown film. These residues were purified by column chromatography on silica gel, first eluting with copious CH₂Cl₂ to remove residual fluorescent BODIPY impurities. After all BODIPY impurities had eluted (as judged by UV–vis spectroscopy), the desired product was eluted as a dark brown solution using CH₂Cl₂/THF (20:1), characterized by optical transitions at 347 nm (BODIPY), 435 and 483 nm (Soret peaks), 512 nm (BODIPY), 611 and 678 nm (Q bands). The free-base porphyrin was converted to the dication by washing with 5% aq HCl (2 \times 50 mL) and water (1 \times 75 mL). The organics were dried (MgSO₄), filtered, and concentrated by rotary evaporation to a brown film. Porphyrin **2** was obtained in pure form as the green-brown bis(hydrochloride) salt by precipitation from CH₂Cl₂ upon layering with Et₂O (76 mg, 35%). UV–vis (CH₂Cl₂) λ_{max} (log ϵ): 354 (4.67), 481 (5.41), 513 (5.27), 623 (4.03), 680 (4.45). ¹H NMR (CDCl₃): δ 8.54 (d, ³J_{HH} = 8 Hz, 8H, Ar-H), 8.02 (d, ³J_{HH} = 8 Hz, 8H, Ar-H), 6.94 (d, ³J_{HH} = 4 Hz, 8H, BODIPY Ar-H), 6.44 (d, ³J_{HH} = 4 Hz, 8H, BODIPY Ar-H), 2.77 (s, 24H, BODIPY -CH₃), 2.62 (dt, ²J_{HH} = 17 Hz, ³J_{HH} = 6 Hz, 8H, -CH₂), 2.16 (dt, ²J_{HH} = 17 Hz, ³J_{HH} = 6 Hz, 8H, -CH₂), 1.80 (m, 8H, -CH₂), 1.26 (m, 8H, -CH₂), 0.86 (s, 4H, -NH). ¹³C NMR (CDCl₃): δ 158.4, 143.8, 141.3, 139.7, 136.2, 135.5, 135.2, 134.5, 130.6, 130.1, 120.0, 117.1, 24.7, 22.4, 15.1. MALDI: *m/z* for C₁₀₄H₉₀B₄F₈N₁₂ calcd 1703.8, found 1702.1.

Platinum Cyclohexenoporphyrin 3 [Pt(^{BDP}TPCHP)]. Platinum(II) chloride (40 mg, 0.15 mmol) was added to dry, degassed benzonitrile (40 mL), and the mixture was heated with stirring under N₂ at 100 °C, causing the platinum salts to dissolve as the solution turned yellow. The cyclohexenoporphyrin dication 2·(HCl)₂ (40 mg, 0.023 mmol) was added as a solid, and the resulting solution was heated with stirring at reflux for 3 h. The mixture was cooled to ambient temperature and benzonitrile removed by vacuum distillation. The residues were dissolved in CH₂Cl₂ and filtered to remove solids. The filtrate was dried in vacuo to afford a dark brown powder, which was further purified by washing with methanol (3 \times 10 mL). The powder was subjected to column chromatography (SiO₂ gel, CH₂Cl₂ eluent), and the cleanest fractions were combined, dried by rotary evaporation, and crystallized as green plates by layering a concentrated solution of **3** in CH₂Cl₂ with Et₂O (33 mg, 69%). UV–vis (CH₂Cl₂) λ_{max} (log ϵ): 340 (4.8), 410 (5.4), 512 (5.5), 569, (4.4). ¹H NMR (CDCl₃): δ 8.22 (d, *J* = 8 Hz, 8H, phenyl Ar-H), 7.83 (d, *J* = 8 Hz, 8H, phenyl Ar-H), 6.94 (d, *J* = 4 Hz, 8H, BODIPY Ar-H), 6.41 (d, *J* = 4 Hz, 8H, BODIPY Ar-H), 2.75 (s, 24H, -CH₃), 2.48 (s, 16H, -CH₂), 1.61 (s, 16H, -CH₂). ¹³C NMR (CDCl₃): δ 158.2, 143.0, 140.2, 139.8, 134.9, 134.3, 133.9, 133.8, 130.2, 129.8, 119.9, 118.7, 26.9, 23.7, 15.2. MALDI: *m/z* for C₁₀₄H₈₈B₄F₈N₁₂Pt calcd 1895.7, found 1894.1.

Platinum Benzoporphyrin 4 [Pt(^{BDP}TPBP)]. Platinum cyclohexenoporphyrin **3** (Pt(^{BDP}TPCHP), 33 mg, 0.017 mmol) was dissolved in toluene (30 mL). DDQ (40 mg, 0.18 mmol) was added, and the solution was heated at reflux with stirring for 45 min, causing the color to change from brown to olive. The resulting solution was washed with sodium sulfite (10% aq, 2 \times 50 mL) and brine (1 \times 50 mL), dried (MgSO₄), filtered, and concentrated in vacuo to a dark solid. These dark residues were dissolved in

minimal CHCl₃ (ca. 1 mL), and the solution was layered with Et₂O, causing black solids to precipitate overnight. The compound was purified by an additional precipitation from CH₂Cl₂ with Et₂O, yielding the title compound as a black solid that was isolated by filtration (5 mg, 15%). UV–vis (CH₂Cl₂) λ_{max} (log ϵ): 281 (4.98), 340 (4.83), 433 (5.40), 514 (5.48), 573 (4.34), 619 (5.07). ¹H NMR (CDCl₃): δ 8.45 (d, *J* = 8 Hz, 8H, phenyl Ar-H), 8.06 (d, *J* = 8 Hz, 8H, phenyl Ar-H), 7.33–7.36 (m, 8H, porphyrin Ar-H), 7.24–7.26 (m, 8H, porphyrin Ar-H), 7.16 (d, *J* = 4 Hz, 8H, BODIPY Ar-H), 6.50 (d, *J* = 4 Hz, 8H, BODIPY Ar-H), 2.79 (s, 24H, -CH₃). ¹³C NMR (CDCl₃): δ 158.6, 143.2, 142.0, 137.7, 136.1, 135.4, 134.9, 133.8, 131.6, 130.3, 125.9, 124.3, 120.2, 117.9, 15.3. MALDI: *m/z* for C₁₀₄H₇₂B₄F₈N₁₂Pt calcd 1878.6, found 1878.9.

Femtosecond Transient Absorption Spectroscopy. Femtosecond transient absorption measurements were performed using the output of a Ti:sapphire regenerative amplifier (Coherent Legend, 4 mJ, 35 fs) operating at a 1 kHz repetition rate. ~10% of the amplifier output was used to pump a type II OPA (Spectra Physics OPA-800C) and sum frequency of the signal and residual 800 nm pump generated 3.5 μ J excitation pulses centered at 508 nm with 6.5 nm of bandwidth. Prior to the sample, the excitation pulses were attenuated by a neutral density filter and were focused behind the sample using a 50 cm CaF₂ lens. Assuming a Gaussian profile, the pump spot size at the sample had a fwhm of 380 μ m. Probe pulses were generated by focusing a small amount of the amplifier output into a rotating CaF₂ plate, yielding a supercontinuum spanning the range of 320–950 nm. A pair of off-axis aluminum parabolic mirrors collimated the supercontinuum probe and focused it into the sample.

The sample consisting of **4** dissolved in toluene solution was held in a 1-cm path length quartz cuvette under a deoxygenated atmosphere and had a peak optical density of 0.17 at 517 nm. The polarization of the pump and probe were set perpendicular to one another, which allowed for the suppression of scatter by passing the probe light transmitted by the sample through a polarizer prior to detection. A spectrograph (Oriel MS127I) was used to disperse the supercontinuum probe onto a 256 pixel silicon diode array (Hamamatsu), allowing multiplex detection of the transmitted probe as a function of wavelength. Pump induced changes in the probe were determined by using an optical chopper to block every other pump pulse. At early time delays, a strong nonresonant signal from the sample cell and solvent is observed and relaxes within 300 fs. Careful measurement of this nonresonant signal enabled its partial subtraction from the transient data and allowed the data to be corrected for the temporal dispersion of the supercontinuum probe resulting from propagation through the CaF₂ plate and sample.

The data presented in the text were measured for a pump fluence of 150 μ J/cm². Based on the measured absorption cross section of **4**, at this fluence we expect at most only a single excitation per molecule. However, to verify that annihilation processes do not contribute to the signal, we also measured transient spectra using a pump fluence of 75 μ J/cm² and found that the signal scaled linearly between the two data sets.

Nanosecond Transient Absorption Spectroscopy. Time-resolved spectroscopic measurements were carried out at the Beckman Institute Laser Resource Center. Samples were degassed prior to experiments by three freeze–pump–thaw cycles. Laser excitation was achieved with 8-ns pulses from a 10 Hz Q-switched Nd:YAG laser (Spectra-Physics Quanta-Ray PRO-Series). The third harmonic was used to pump an optical parametric oscillator (Spectra-Physics Quanta-Ray MOPO-700) that provided excitation at 487 nm.

A pulsed 75-W arc lamp (PTI model A 1010) supplied probe light for transient absorption measurements. A double monochromator (Instruments SA DH-10) with 1 mm slits was used to select probe wavelengths. Transmitted light was detected with a photomultiplier tube (PMT, Hamamatsu R928). The PMT current was amplified and recorded with a transient digitizer (Tektronix DSA

602). Short and long pass filters were employed to remove scattered excitation light. Decay kinetics were averaged over 500 laser pulses.

All instruments and electronics in these systems were controlled by software written in LabVIEW (National Instruments). Data manipulation was performed with MATLAB R2008a (Mathworks, Inc.) and graphed with Origin software.

Acknowledgment. Funding for this research was provided by the Center for Advanced Molecular Photovoltaics (CAMP) (KUS-C1-015-21) of the King Abdullah University of Science and Technology (KAUST) and the Global Photonic Corporation. The quantification of absorbance at AM1.5G illumination and femtosecond transient absorption measurements were carried out with support from the Department of Energy's Energy Frontier Research Center program (Center for Energy Nanoscience, Award DE-SC0001011). S.T.R. acknowledges support from the National Science Foundation in the form of an ACC-F fellowship (CHE-

0937015), and A.C.D. acknowledges support from the NSF Center for Chemical Innovation (CCI Powering the Planet, Grants CHE-0802907 and CHE-0947829). We are also grateful to Dr. Jay Winkler and the Beckman Institute Laser Resource Center at the California Institute of Technology for assistance with nanosecond transient absorption measurements. We dedicate this manuscript to Professor Harry B. Gray, pioneer of inorganic photochemistry, on the occasion of his 75th birthday.

Supporting Information Available: Derivation of eq 1; ^1H NMR spectrum of **4**; absorption and photoluminescence spectra for **3**, **4**, and model complexes; femtosecond-resolved transient absorption spectra for **3**. This material is available free of charge via the Internet at <http://pubs.acs.org>.

JA108493B